Comparison of the Effects of Saccharide Binding and Crystallization on the Zinc Transition-Metal Site of Concanavalin A†

S.-L. Lin,‡,§ E. A. Stern,*,‡ A. J. Kalb (Gilboa),∥ and Y. Zhang‡

Department of Physics FM-15, University of Washington, Seattle, Washington 98195, and Department of Biophysics, Weizmann Institute of Science, Rehovoth, Israel

Received May 10, 1991; Revised Manuscript Received July 25, 1991

ABSTRACT: The Zn site in concanavalin A *solution* was studied by X-ray absorption fine structure spectroscopy (XAFS) with and without the saccharide methyl α-D-glucoside (aMG) bound to the protein. No structural change occurs in the metal-binding site when the saccharide is bound to the protein. There is, however, evidence for structural change remote from the metal site. This is in contrast to the significant changes that we have previously found to occur in the near neighborhood of the Zn atom when an aqueous solution of Zn concanavalin A crystallizes. We propose a structural explanation of these facts based on the known crystal structure of concanavalin A.

Concanavalin A is a saccharide-binding protein from jack bean. It is capable of selectively binding to D-mannosides and D-glucosides (Yariv et al., 1968; Goldstein & Hayes, 1978). It is of fundamental importance to characterize the conformation of the protein and its saccharide complexes in order to understand the mechanism of binding. Concanavalin A has two metal sites, one of which is a transition-metal site and the other of which contains Ca. Both of the sites must be occupied for concanavalin A to bind saccharide (Kalb & Levitzki, 1968). The structure of the saccharide-binding site was solved recently by X-ray crystallography on a complex of concanavalin A with methyl α-mannopyranoside (aMM) (Derewenda et al., 1989). The site is located in a groove on the protein surface, along the extension of the straight line connecting the two metal atoms. The center of the bound saccharide is 12.8 Å from the transition metal and 8.7 Å from the calcium ion. Several of the amino acid residues that are involved in the interaction between the protein and the saccharide are also involved in binding of calcium. The calcium site, in turn, has several ligands that are involved in binding the transition metal. It is therefore feasible that perturbation of the saccharide-binding site may be transmitted to the transition-metal site, especially in view of our recent finding (Lin et al., 1990, 1991) that the Zn-binding site is susceptible to the perturbation of the surface of the protein molecule caused by crystallization.

Several spectroscopic studies have been reported on the effect of saccharide binding upon the transition-binding site (Kalb & Pecht, 1973; Meirovitch & Kalb, 1973; Meirovitch et al., 1974; Brewer et al., 1973; Grimaldi & Sykes, 1975; Alter & Magnuson, 1974). None of these have found evidence for structural change in the environment of the metal. The high sensitivity of XAFS to structural change in the near vicinity of the metal ion as well as the possibility of quantitative structural interpretation of the extended XAFS region have led us to reopen this question.

Experimental Procedures and Results

Saccharide-free concanavalin A was obtained from a commercial supplier (Bioyeda, Israel). Solution samples were prepared by removal of the naturally occurring metal by acid treatment and addition at pH 5.2 in 1 M NaCl of Zn and Ca salts (Shoham et al., 1973). Zn then occupies the transition-metal site and Ca the other (Kalb & Levitzki, 1968). The Zn–protein concentration was 2 mM or more, while the free Zn concentration in solution was 0.1 mM. The complex with aMG was prepared by addition of the saccharide to a final concentration of 0.1 M to achieve saturation of the saccharide-binding site. XAFS experiments were performed at the NSLS X-11 beam line with a double Si(111) crystal monochromator. The protein samples were measured at the Zn K-edge in a fluorescence mode at ambient temperatures and processed by standard methods to obtain the normalized XAFS spectra χ of the first shell (Stern & Heald, 1983). Such XAFS spectra contain detailed structural information on the ligands surrounding the Zn atom, namely, types, numbers, average bond lengths, and disorder about the average.

Comparison of the spectra between the aMG-bound and aMG-free samples was done by two methods. One was the ln ratio method and the other was a direct substraction of the XAFS spectra. In the ln ratio method the ratio of amplitudes of the first-shell XAFS spectra $\chi(k)$ and the difference of their phases are given by

$$\frac{A_1}{A_2} = \frac{N_1}{N_2}\frac{R_2^2}{R_1^2}\exp(-2k^2\Delta\sigma^2) \quad (1)$$

$$\phi_1 - \phi_2 = 2k\Delta R \quad (2)$$

where A_1 and A_2 are the amplitudes and ϕ_1 and ϕ_2 are the phases of the two samples with and without aMG, repectively. N_1 and N_2 are the coordination numbers of the Zn ion, R_1 and R_2 are the average ligand bond lengths, $\Delta R = R_1 - R_2$, and $\Delta\sigma^2$ is the difference in the mean squared disorder in the bond lengths of the two species. The wavenumber k of the K-shell excited photoelectron is given in reciprocal angstroms by $k^2 = 0.263(E - E_0)$, where E is the X-ray energy and E_0 is the core binding energy, both in electron volts. E_0 is chosen at the energy value halfway up the edge step.

Figure 1 shows the near-edge region of the two spectra. The near-edge region is sensitive to the arrangement of atoms up to about 10 Å from the Zn site. In contrast, the extended XAFS data of Figure 2 is sensitive to changes only within about 4 Å, as shown in Figure 3. Figure 2 shows the $k^3\chi(k)$ spectra between $k = 0.5$ and 11 Å^{-1}. Although the aMG-

† This work was funded by NSF under Grant DMB-8613948.

‡ University of Washington.

§ Present address: Department of Biochemistry and Cell Biology, Rice University, P.O. Box 1892, Houston, TX 77251.

∥ Weizmann Institute of Science.

0006-2960/91/0430-9705$02.50/0

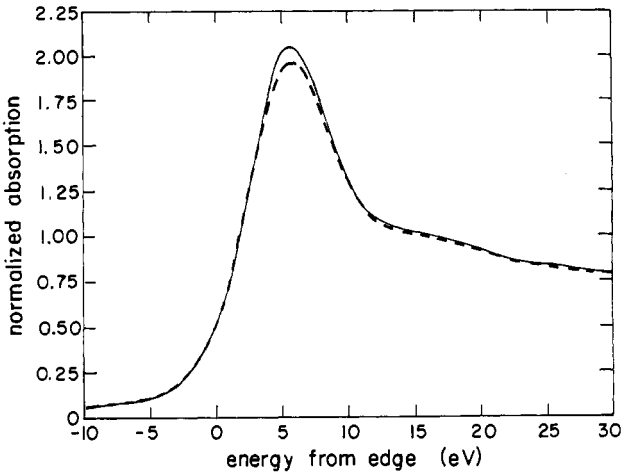

FIGURE 1: Near-edge spectra of the K-edge of the Zn atom in the protein without aMG (dashed line) and with aMG bound (solid line). The noise in the data is about a line width.

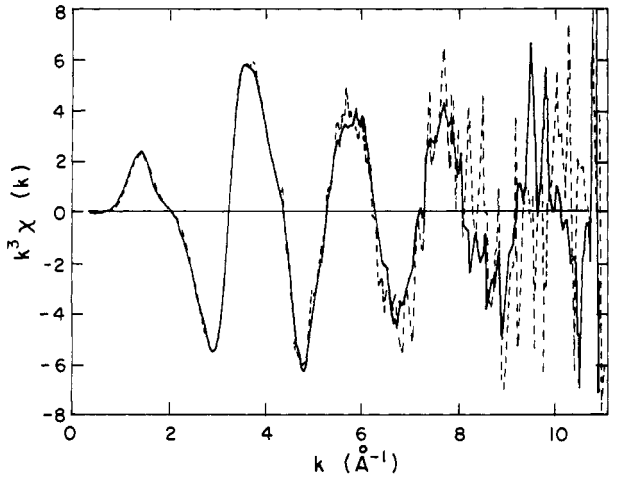

FIGURE 2: Plots of $k^3\chi(k)$ of the protein without aMG (dashed line) and with aMG bound (solid line) for the K-edge of the Zn atom.

bound spectrum is quite noisy above 8 Å^{-1}, the spectra show that the two species are similar to one another. The magnitudes of the Fourier transform of $k^3\chi(k)$ of both samples, obtained by using a window with vertical ends between k = 2 and 8 Å^{-1}, are shown in Figure 3.

To obtain a quantitative analysis the first-shell spectra were isolated in the Fourier transforms by a filtering window whose half-height points are at R = 1.04 and 2.11 Å with Hanning tapers of width 0.4 Å on both sides and were inversely Fourier transformed back to k-space. Equations 1 and 2 were then applied to compare the two species, and the results are plotted in Figure 4. These results for concanavalin A solution with aMG compared to the aMG-free one give

$$N1/N2 = 0.98\ (6) \quad \Delta\sigma^2 = -0.0001\ (14)\ \text{Å}^2 \quad \Delta R = 0.007\ (14)\ \text{Å}$$

They indicate that aMG binding induces no structural changes in the first coordination shell of the Zn site within uncertainties.

To verify that no significant differences exist, we subtract the two $k^3\chi(k)$ spectra from one another and compare this difference spectrum in Figure 5 with the difference in spectra obtained on the same sample but in independent scans. Such a difference indicates the noise introduced by the measurement. Averaging the spectra decreases the noise by the square root of the number of spectra involved. Taking this into account, the differences found in the full spectra between the protein

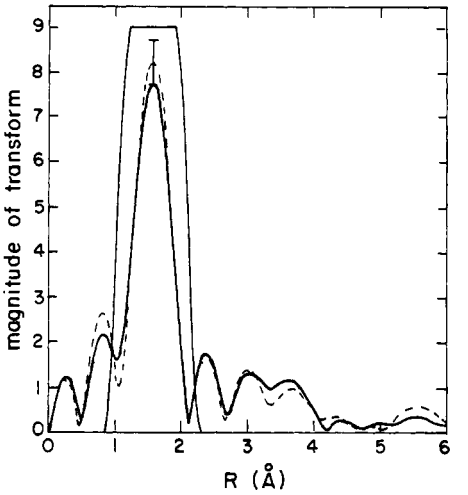

FIGURE 3: Magnitude of the Fourier transform of $k^3\chi(k)$ between k = 2 and 8 Å^{-1}. The cases with aMG bound (solid line) and without (dashed line) are shown. The bar at the peak indicates the uncertainty introduced by the noise in the measurement, which is dominated by the aMG-bound data.

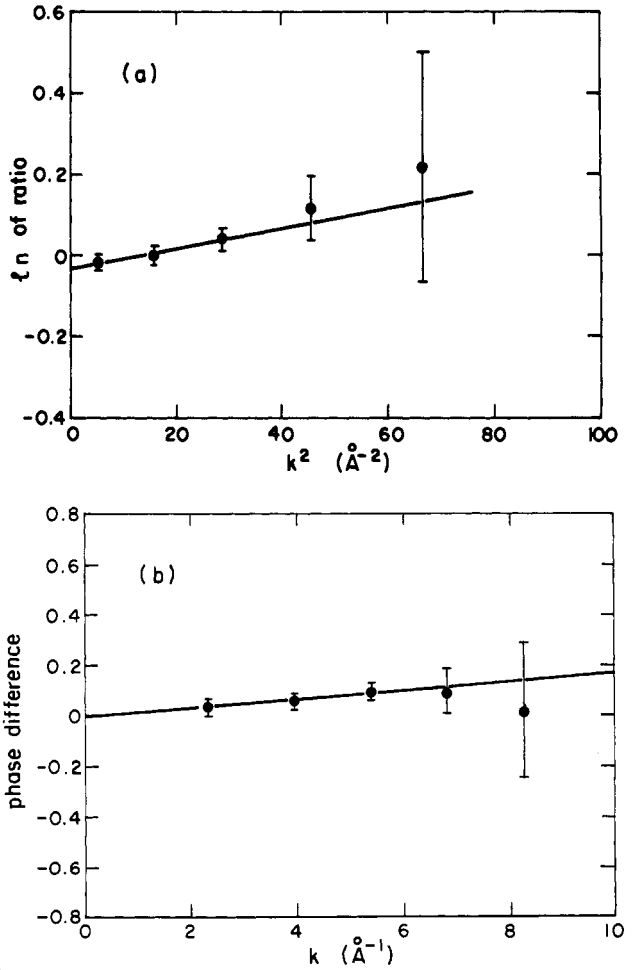

FIGURE 4: (a) Ln ratio of amplitudes and (b) difference in phase in radians between the aMG-bound and aMG-free proteins.

with and without bound aMG are within the uncertainties, indicating no significant differences between the two samples out to the distance where there is significant XAFS structure as seen in Figure 3, namely, 4 Å.

However, the near-edge spectra of Figure 1 have some significant differences. The difference between the near-edge spectra of the protein with and without bound aMG is much

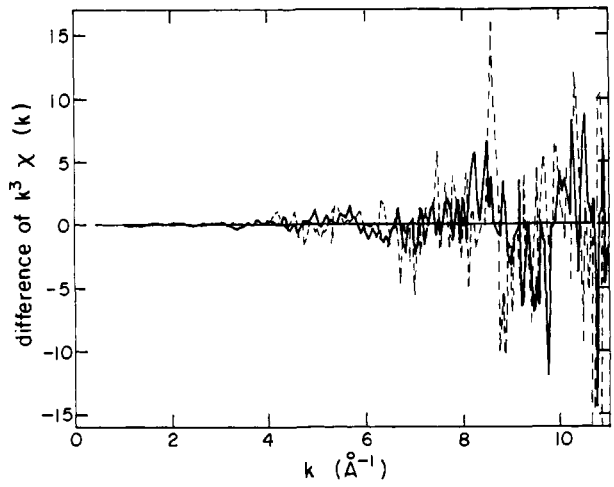

FIGURE 5: Difference in $k^3\chi(k)$ spectra between the protein with and without aMG bound (dashed line) and between two independent scans of the aMG-bound data (solid line).

larger than the measurement fluctuations, which are within the width of the curve. This indicates some change in the protein conformation when aMG binds. Since no change was found in the first neighbors to high accuracy and no change was detected beyond (up to about 4 Å) with less sensitivity, changes indicated by the differences in the near-edge spectra must originate from protein conformations beyond about 4 Å from the Zn site.

Discussion and Conclusions

Our results show that the aMG binding interaction in solution has no significant effect on a neighborhood within 4 Å of the Zn site. This is in contrast with our previous finding that, on crystallization of the saccharide-free protein, the Zn atom loses one N and one O out of six ligands (Lin et al., 1990, 1991). Clearly, this change is brought about by the intermolecular forces of crystallization. In protein crystals, packing forces are generally assumed to be weak. However, the actual interaction on the contact areas binding the molecules together may be rather strong, because they usually span only a small percentage of the protein surface, as is the case for concanavalin A crystals. The X-ray structure of saccharide-free concanavalin A with Mn in the transition-metal site instead of Zn shows that there are three intermolecular contact areas located near residues Asp16, Leu198, and Pro222 (Hardman & Ainsworth, 1972). In this structure the Mn is six-coordinated similar to that found in the *solution* form of Zn concanavalin A. We assume that the environment around the six-coordinated Zn in *solution* is the same as that around the Mn in the crystal, and we suggest how the intermolecular forces of crystallization will destabilize the structure and change the coordination around the Zn to four. Around the contact regions in the crystal, the protein components may be under great stress in fitting into the crystal lattice. The metal sites are located right under a flap consisting of a loop shown by the thick lines in Figure 6 that doubles back on itself and contains, besides Asp16, the other residues Tyr12, Asn14, Asp19, and His24, which provide five of the ligands of the two metal atoms. The loss of the N ligand at the Zn site on crystallization indicates that the histidine residue detaches, disconnecting from the Zn that portion of the loop containing the His24. The closest residue to His24 that is also connected to the same portion of the loop (the upper portion in Figure 6) is Asp19, which donates one oxygen to the Zn metal atom. If the assumption is made that the oxygen ligand that is lost on crystallization is from Asp19, then the two ligands that attach the upper portion of the loop to the metal atoms are disconnected, allowing that portion of the loop to change its conformation. The asymmetry in the four remaining bonds surrounding the Zn can be accommodated by the motion of its two H_2O ligands.

This could provide a resonable mechanism for transmitting the stress imposed by the intermolecular contacts to the transition-metal-binding site, particularly because the loop is outside of the rigid β-sheet core of the protein and may be expected to be relatively flexible. This stress directs the largest resulting strain along the path of least resistance, i.e., the relatively flexible loop, which acts as the conduit to the metal site.

The crystallization effect indicates that the transition-metal site is sensitive to external forces and conformational changes of the protein. The nature of saccharide binding may therefore be monitored at this site, considering its closeness to the saccharide binding site both in space and in connectivity. In solution, when saccharide binding occurs, the binding site is not in contact with an adjacent protein molecule, in contrast

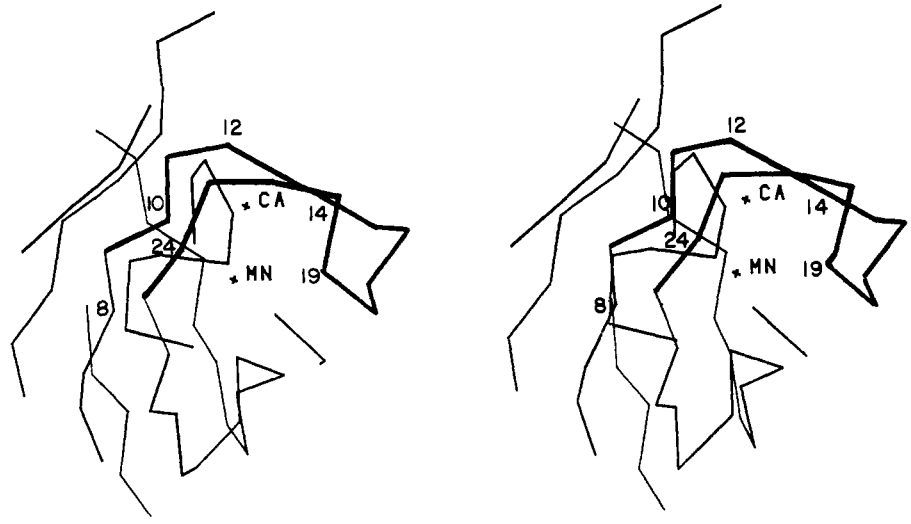

FIGURE 6: Stereo couple of the vicinity of the metal sites for Mn–Ca concanavalin A as determined by the crystal structure analysis of Hardman and Ainsworth (1972). Only the backbone and the metal sites of the portion of the molecule centered around the Mn atom are shown. The α-carbons of the residues that attach the flap to the metal atoms are indicated by their residue numbers. This restricted view cuts out portions of the molecule below and to the left of the Mn site. The flap above the Mn site is at the surface of the molecule and is highlighted by the thicker lines.

to the crystallized protein. What XAFS probes is any structural alteration caused by the binding process that transmits to the transition-metal site. The null effect in the immediate neighborhood of the transition metal proves that the perturbation is transmitted more weakly than in the more rigid crystal. In particular, it does not cause the substantial conformational change of the putative flap rearrangement. Thus, the saccharide binding mechanism in solution does not involve large-scale binding-induced conformational changes in the protein but is localized to the binding-site vicinity.

This suggestion is consistent with the structure of the saccharide-binding site determined by X-ray crystallography (Derewenda et al., 1989). The binding site consists of four arms of exposed loops of the protein. In the bound complex the saccharide resides in the groove formed by the loops. The loops are relatively flexible structures that provide the mechanism of low-barrier structural alterations in the unconstrained environment of the solution. Structural perturbations can be easily relieved by localized adjustments of the portions of the loops bathed in solution, minimizing internal transmission of stress. In the absence of saccharide, the loops may bind to water molecules, lessening the perturbation induced by the saccharide release.

In conclusion, it is suggested that the stresses induced by the intermolecular contact forces at Asp16 combined with the rigidity of the constraints of the lattice are transmitted into the interior, causing the flexible flap held in place by the metal atoms to disconnect from the Zn atom with an attendant conformational change as the protein crystallizes. No such conformational modification occurs in solution because of the absence of the intermolecular contacts. The binding stresses induced by the saccharide in solution, although also located near the metal atoms, can be limited to the vicinity of the binding site because the protein in solution has none of the crystal lattice constraints and can easily relax. This greater rigidity of the protein in the crystal lattice may have other important consequences that may significantly modify the protein properties in other cases.

ACKNOWLEDGMENTS

The help of Professor Ronald Stenkamp in producing Figure 6 is gratefully appreciated.

Registry No. aMG, 97-30-3; Zn, 7440-66-6; concanavalin A, 11028-71-0.

REFERENCES

Alter, G. M., & Magnuson, J. A. (1974) *Biochemistry 13*, 4038–4045.

Brewer, C. F., Sternlicht, H., Marcus, D. M., & Grollman, A. P. (1973) *Biochemistry 12*, 4448–4457.

Derewenda, Z., Yariv, J., Helliwell, J. R., Kalb (Gilboa), A. J., Dodson, E. J., Papiz, M. Z., Wan, T., & Campbell, J. (1989) *EMBO J. 8*, 2189–2193.

Goldstein, I. J., & Hayes, C. E. (1978) *Adv. Carbohydr. Chem. Biochem. 35*, 127–340.

Grimaldi, J. J., & Sykes, B. D. (1975) *J. Biol. Chem. 250*, 1618–1624.

Hardman, K. D., & Ainsworth, C. F. (1972) *Biochemistry 11*, 4910–4919.

Kalb, A. J., & Levitzki, A. (1968) *Biochem. J. 109*, 669–672.

Kalb, A. J. & Pecht, I. (1973) *Biochim. Biophys Acta 303*, 264.

Lin, S.-L., Stern, E. A., Kalb (Gilboa), A. J., & Zhang, Y. (1990) *Biochemistry 29*, 3599–3603.

Lin, S.-L., Stern, E. A., Kalb (Gilboa), A. J., & Zhang, Y. (1991) *Biochemistry 30*, 2323–2332.

Meirovitch, E., & Kalb, A. J. (1973) *Biochim. Biophys. Acta 303*, 258.

Meirovitch, E., Luz, Z., & Kalb, A. J. (1974) *J. Am. Chem. Soc. 96*, 7542.

Shoham, M., Kalb (Gilboa), A. J., & Pecht, I. (1973) *Biochemistry 12*, 1914–1917.

Stern, E. A., & Heald, S. M. (1983) *Handbook on Synchrotron Radiation*, (Koch, E. E., Ed.) Vol. 1, pp 955–1014, North-Holland Publishing Co., Amsterdam.

Yariv, J., Kalb, A. J., & Levitzki, A. (1968) *Biochim. Biophys. Acta 165*, 303–305.